

Article

A Methodology Linking Tamping Processes and Railway Track Behaviour

Stefan Offenbacher ^{1,*}, Christian Koczwar ² , Matthias Landgraf ¹  and Stefan Marschnig ¹ ¹ Institute of Railway Engineering and Transport Economy, Graz University of Technology, 8010 Graz, Austria² Plasser & Theurer, 4021 Linz, Austria

* Correspondence: stefan.offenbacher@tugraz.at

Abstract: Today's railway transport is built upon high-performance infrastructure. Cost-effective yet sustainable infrastructure presumes tracks with a precise and durable geometry. At ballasted tracks, the geometry is created and restored through tamping machines, which position the track panel and compact the ballast beneath the sleepers. It is commonly agreed that the ballast compaction plays an important role in the long-term stability of the track. Yet, there is no method available which allows a direct correlation between the compactness of the ballast and the stability of the track geometry. Available studies either model track behaviour without considering the bedding, or analyse ballast compactness locally while disregarding its influence on the track geometry. This paper presents a new methodology which establishes a relation between these two topics—ballast compaction during tamping and subsequent track behaviour. A state-of-the-art tamping machine has been equipped with an experimental measurement setup, constantly recording relevant data during every tamping process. These data can be used to derive an indication for the achieved compaction under every sleeper. Utilising the tamping machine's internal measuring system for track geometry documentation, every tamping process (every sleeper) is assigned to the precise position along the track. The data set is merged and synchronised with regular track geometry measurements of the infrastructure manager. The result is a comprehensive data set which allows precise analyses between tamping machine measurements and track behaviour. This data set provides the foundation for future research, aiming towards a better understanding of the tamping process and its influence on the quality and durability of the established track geometry.



Citation: Offenbacher, S.; Koczwar, C.; Landgraf, M.; Marschnig, S. A Methodology Linking Tamping Processes and Railway Track Behaviour. *Appl. Sci.* **2023**, *13*, 2137. <https://doi.org/10.3390/app13042137>

Academic Editor: Sanghyun Choi

Received: 10 January 2023

Revised: 1 February 2023

Accepted: 5 February 2023

Published: 7 February 2023



Copyright: © 2023 by the authors. Licensee MDPI, Basel, Switzerland. This article is an open access article distributed under the terms and conditions of the Creative Commons Attribution (CC BY) license (<https://creativecommons.org/licenses/by/4.0/>).

Keywords: track quality; track behaviour; tamping process; ballast compaction; ballast condition

1. Introduction

Modern railway transport—passengers or goods—relies on railway tracks that can cope with high traffic loads and high train speeds, while maintaining their functionality over a long period of time. One of the most important aspects in that regard is the evenness of the track, i.e., the track geometry. A precise track geometry not only enables high speeds, but also keeps dynamic loads at a minimum, which preserves the entire track structure and prolongs its service life. Geometrical defects, on the other hand, limit the permitted speed and increase dynamic effects, thus accelerating the decay of the track geometry quality. If not corrected in time, severe geometrical defects will eventually become safety hazards [1,2].

The geometry of ballasted tracks is nowadays typically created and restored by use of mechanised tamping machines. During a tamping process, the tamping machine brings the track panel (rails + sleepers) to a pre-defined position by lifting it vertically and shifting it horizontally. Subsequently, tamping tines are lowered into the ballast bed, filling the arisen voids and compacting the ballast underneath the sleepers through a closing movement. In case the tamping section lacks ballast or a high lift of the track panel is required, additional ballast needs to be cast prior to the tamping operation. Tamping can also be undertaken manually with hand-held devices; however, the scope of this paper only

comprises mechanised tamping. As levelling-lining-tamping defines the track geometry, this process is highly relevant for the quality and longevity of the tracks. Accordingly, tamping operations affect the life cycle costs of the entire railway infrastructure to a significant extent [3–5]. Hence, a lot of research has been conducted in the field of track deterioration modelling and maintenance planning, oftentimes focusing on the prediction of the optimal point in time for the next tamping intervention (e.g., [6–9]). Some models also expand the projection period beyond the next tamping operation, which requires estimating the new track geometry quality after the next tamping operation. Typically, the track behaviour and the ultimate quality before tamping are considered decisive for the track quality after tamping [9–11]. However, this approach compulsorily implicates uncertainties in the prediction as the influence of the tamping process itself is entirely disregarded. Crucial parameters of the tamping processes—e.g., lifting of the track panel, number of squeezing processes per sleeper, squeezing time—have never been considered in previous investigations. Yet, it is generally assumed that the working quality, and the ballast compaction achieved by the tamping tools in particular, strongly affects the stability of the tracks.

This paper presents a novel methodology which creates a relation between the tamping process and the achieved ballast compaction on the one hand and the established track geometry quality on the other hand. Advancements in sensor technology allow for the recording of measurement data directly at the tamping tools during every tamping process. This information is then linked to the quality of the established track geometry. The result of this paper is a comprehensive data set containing sleeper-specific tamping machine measurements as well as information on the track behaviour at the respective location (Figure 1). Future analyses based on this data set will allow the determination of ballast compaction and ballast condition indicators from the tamping data and show the effect of the compaction on the sustainability of the established track geometry. This integrated analysis of sleeper-specific tamping machine measurements and subsequent track behaviour provides the foundation for optimisation and automation of the tamping process, which in turn can improve the quality and durability of railway tracks.

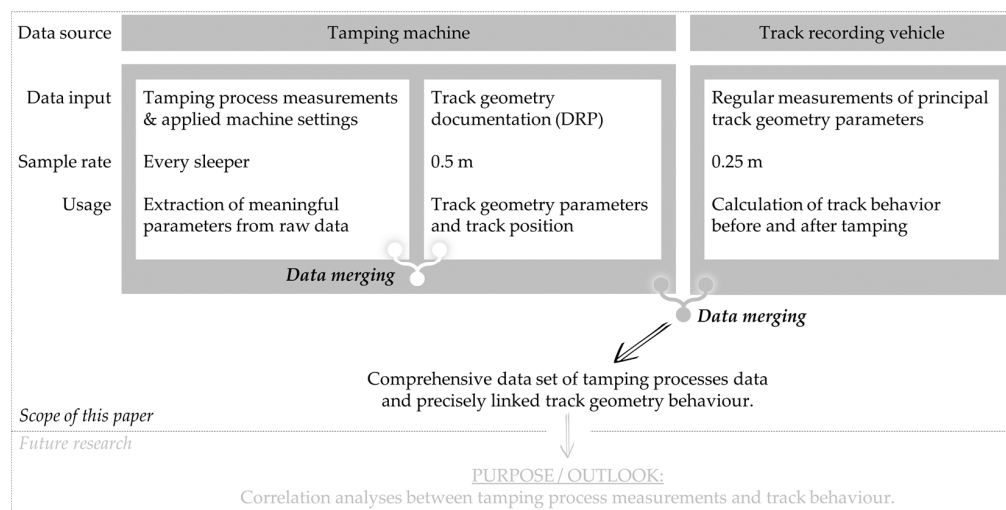


Figure 1. Concept and scope of this paper.

2. Basics of Track Geometry

Railway tracks need to be regularly monitored and inspected in accordance with legal standards (e.g., European Standards) and inspection plans of the infrastructure manager. The particular focus of the monitoring process lies on the principal parameters of the track geometry, as defined in the European Standard EN 13848-1 [12]: Longitudinal level, alignment, gauge, cross level, and twist (illustrated in Figure 2). Longitudinal level and alignment represent the unevenness of each rail in the vertical and horizontal plane, ex-

pressed via three wavelength ranges D1 (3–25 m), D2 (25–70 m), and D3 (longitudinal level: 70–150 m, alignment: 70–200 m). Optionally, short waves (D0: 1–5 m) may also be evaluated, as these are attributed to creating high dynamic loads. Gauge is defined as the shortest distance between both rails, measured 14 mm below the rail heads. Cross level is the relative vertical position of the two rails, while twist expresses the change of the cross level over a defined distance.

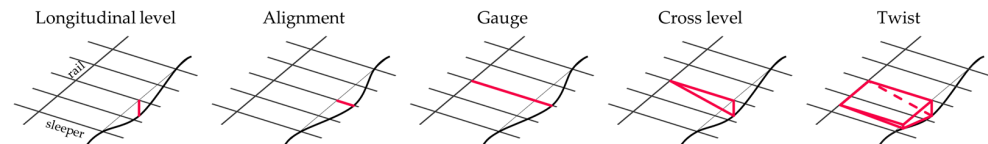


Figure 2. Principal track geometry parameters according to EN 13848-1; red lines illustrate the deviation from the ideal geometry.

2.1. Track Quality Indices

The principal track geometry parameters are critical for safe railway operation, and the respective measurement signals must not exceed defined threshold levels (intermediate action level, IAL) at any point along the track [13]. However, while these geometry signals are appropriate for comparison with threshold values, they are less suited to describe the general track quality and observe its behaviour over a longer section. For this purpose, track quality indices (TQIs) have been established [14–16]. A track quality index considers all data points of a track geometry signal within a defined track segment (“window”) and represents the average track condition of this segment by a single value. The most widely used index to describe the quality of a track is the standard deviation (*SD*) of the longitudinal level [16], calculated according to Equation (1) [17]:

$$SD = \sqrt{\frac{\sum_{i=1}^n (x_i - \bar{x})^2}{N - 1}} \quad (1)$$

Track quality indices based on an individual track geometry parameter are typically used for maintenance planning; the selected parameter already indicates the required maintenance work (e.g., a poor standard deviation of the longitudinal level triggers levelling-lining-tamping) [5,9]. Single-parameter indices can also be combined to create a holistic track quality index, representing the overall track geometry condition. A holistic TQI, however, is not appropriate to predict maintenance tasks, as it is impossible to identify the source of a quality issue, thus the required maintenance type cannot be derived from the aggregated quality figure. An overview of existing track quality indices can be found in [16].

The magnitude of any track quality index at a certain cross section is severely affected by two calculation parameters: (i) the calculation type (discrete or moving) and (ii) the window length [16,18]. (i) A discrete calculation delivers a continuous value for the entire considered window, i.e., the respective track segment. On the plus side, segments in need of maintenance can be easily identified. A downside is that the location of the segments (start and end point) has a strong effect on the results. For example, a severe isolated defect at the cut-off point between two segments affects both; if the segments are shifted by a small distance, the isolated defect will have a stronger influence on one segment while not affecting the other [18]. A moving calculation assigns the calculated track quality value of the current window to its centre point, before the window is shifted by one data break and the calculation is repeated. Thus, a moving TQI reflects the input signal better than a discrete TQI and is considered more suitable to represent the track quality [18]. (ii) The window length defines how many data points are included in the calculation of a TQI. Larger windows have a smoothing effect, while shorter windows emphasise local defects [16]. Typical window lengths are 200 m [17] and 100 m (applied at Austrian Federal Railways and Swiss Federal Railways, for example [19,20]).

2.2. Track Behaviour

The behaviour of railway tracks over time (or cumulated track load) can be analysed on a global level or on a detailed level. Global analyses consider the entire service life, from the installation of the track to its dismantlement or renewal [21]. Detailed analyses of the track behaviour investigate individual deterioration periods, beginning and ending with a major maintenance activity. It is common practice to confine deterioration periods of ballasted tracks by tamping operations [11,18,22].

Sauni et al. [22] describe the theoretical track behaviour of an individual cross section, based on the longitudinal level, as presented in Figure 3. Immediately after tamping, a rapid deterioration describes initial track settlements, which eventually abate. Subsequently, the deterioration period transitions into its main stage, characterised by a steadily worsening track geometry. In the final phase—which is rarely reached in practice [9,22]—the already poor track quality is subjected to an accelerating rate of geometry deterioration. If the longitudinal level signal itself is analysed rather than a derived track quality index, exponential defect growth can be observed at isolated defects [23].

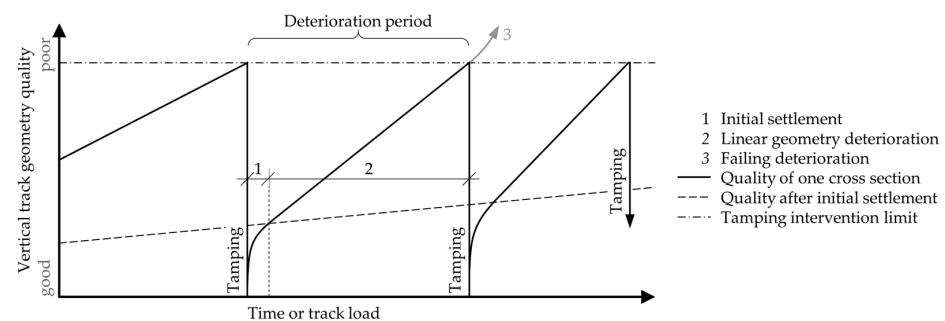


Figure 3. Theoretical track behaviour by means of the vertical track geometry quality.

Numerous models have been established by a variety of researchers to best describe and predict the track behaviour. Neuhold [9] analysed linear, logarithmic, and exponential functions and concluded that all three do occur in practice: The logarithmic function describes initial settlements, the exponential function describes the theoretical end-of-life behaviour, and a linear function is best suited to represent the main phase of the deterioration period. Besides these rather simple functions, many more deterioration and prediction models have been investigated by a large number of researchers. A comprehensive overview of published models is provided by Elkhoury et al. [24] or Soleimanmeigouni et al. [25,26].

3. Principles of Tamping Processes

The creation and correction of the track geometry through tamping machines can be interpreted as sequence of consecutive tamping processes, conducted at every sleeper [27]. Each tamping process consists of multiple phases: (1) lifting and levelling, (2) tamping unit positioning, and (3) the squeezing process [28]. The squeezing process comprises (a) ballast penetration, (b) squeezing movement (which is further subdivided into a filling and compaction process), and (c) raising the tamping unit (Figure 4) [21,28].

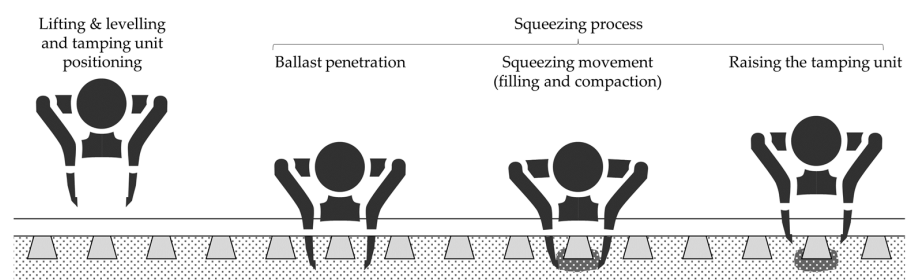


Figure 4. Main phases of a tamping process.

Depending on the lift of the track panel, the track condition, and guidelines of the infrastructure manager (if available), multiple squeezing processes are executed at every sleeper [21,27,29].

3.1. Tamping Parameters

The success of a tamping process, i.e., the stability of the created track geometry, depends on multiple parameters. On the one hand, the condition of the track before the tamping operation, more specifically the geometrical quality of the track and the condition of the ballast, affect the outcome of the tamping work [2,9]. On the other hand, different factors within the realm of the tamping machine are highly important for the quality of the tamping process. Depending on the source, these factors are referred to as working parameters [30], tamping parameters [31], or operating parameters [32]. In this paper they are commonly named tamping parameters:

- Lift of the track panel [30–32];
- Shift of the track panel [30];
- Squeezing time [30–32];
- Tamping depth [30,32];
- Tamping tine oscillation frequency [31,32];
- Tamping tine oscillation amplitude [31,32];
- Squeezing velocity [31,32];
- Squeezing force/pressure [31];
- Number of insertions/interventions [21].

Lift and shift determine how far the track panel is raised vertically and moved horizontally during the tamping process, depending on the deviation of the track panel from its origin position [21]. The oscillation parameters (frequency and amplitude) are usually predefined, ideal values have been established empirically [33] and tested with computer models [34,35]. Other tamping parameters need to be selected carefully by the machine operator, considering the displacement of the track panel and the local track condition. The application of optimal machine settings is crucial to form a well-compacted sleeper bearing [31,32]. A tamping machine may also incorporate additional compaction tools besides the tamping tines, such as ballast shoulder consolidators or dynamic track stabilisers [21]. However, the scope of this paper is confined to the compaction achieved by the tamping tools.

3.2. Compactness of the Ballast

A well-compacted ballast bed is an important factor for the quality and durability of the track geometry [34,36–42]. Different methods have been proposed to assess the compactness of the track ballast. These methods can be summarised as direct measurements, indirect assessments, and computer models and simulations. Direct measurements of the ballast compactness were conducted by Zhou et al. [43] and Liu et al. [40] in the form of the water-filling method. This approach allows a precise calculation of the compactness and its change during tamping (by repeating the experiment afterwards) but implies a disturbance of the ballast matrix at the examination point. Indirect assessments of the ballast compactness were conducted by Barbir et al. [44] and Sysyn et al. [39]. The former analysed measurement data recorded by sensors attached to the tamping tines of a tamping machine, from which they derived parameters indicating the plastic deformation of the ballast matrix, which correlates with the compaction. The latter employed the seismic method, which makes use of the dependence of the wave propagation velocity of an acoustic signal on the compactness of granular matter. Both studies delivered promising results and proofed the applicability of the respective concept. Sysyn et al. [39] note that the quality of the ballast compaction can also be estimated (i.e., indirectly assessed) by the stability of the track geometry (Section 2.2). Computer models and simulations enable sophisticated analyses of the interaction between tamping tools and the bedding. Shi et al. [45] created a model coupling the discrete element method and multibody dynamics.

The model allowed analyses of the ballast compactness in different areas of the track cross section and clearly showed the positive effects of tamping in that regard.

4. Proposed Methodology

Although it is commonly accepted that the compactness of the track ballast is crucially important for the quality and longevity of railway tracks (Section 3.2), there is no study known to the authors providing a direct relation between the two topics. Bottom-up approaches such as the water-filling method [40,43] or seismic method [39] are restricted to the local testing zone; scaling those experiments to larger track sections or even entire railway lines is not feasible. Furthermore, experiments such as those introduced in Section 3.2 limit the scope to the ballast compactness and do not consider the subsequent behaviour of the track geometry. Top-down approaches, i.e., using the track behaviour as indication for the quality of the ballast compaction, are quite vague. The track geometry is influenced by many factors, which (likely) have a larger impact on the geometry quality and long-term stability of the tracks. Among the relevant factors are type of superstructure, line speed, traffic load, alignment, and weather conditions [11,46].

In this paper, we propose a novel methodology which intends to create a relation between the two topics of ballast compaction and track behaviour. Our approach requires measurement data from two different sources: Tamping machine measurements provide the basis to analyse each tamping process individually and derive an indicator for the achieved ballast compaction (Section 4.1) and ballast condition. Track recording vehicle data enable analyses of the initial quality and the behaviour of the track section where said tamping machine is operated (Section 4.2). Subsequently, both data sets need to be carefully joined, so that each tamping process can be assigned the geometric quality and deterioration rate developing at its location (Section 4.3).

4.1. Tamping Data Preparation

The tamping machine measurements used in this study were recorded by the universal single-sleeper tamping machine Unimat 09-4x4/4S E³ by Plasser & Theurer (Vienna, Austria), which mainly operates in the networks of the Austrian Federal Railways (OeBB) and Swiss Federal Railways (SBB). The machines' tamping unit comprises four tamping unit segments, two of which are located at each side of the track. One tamping unit segment sits at the outer side of the rail (towards the ballast shoulder) and one at the inner side (towards the track centre), respectively. Every tamping unit segment consists of two tamping arms—one before the sleeper and one behind—with two tamping tines each. The tamping machine has been equipped with an experimental measurement setup: strain gauges are fitted into the tamping tines, angle encoders and accelerometers are attached to the frames of the tamping unit segments, and pressure sensors are incorporated in the hydraulic system of the tamping unit segments (Figure 5). This sensor system continuously records a large quantity of parameters during every working shift of the tamping machine. Of particular relevance for the present study are the moving distance of the tamping arms and the normal forces in the tamping tines during the squeezing movement. The movements of the tamping arms are traced by the angle encoders; the forces are recorded by the strain gauges and additionally calculated from pressure measurements. The sample rate of said measurement data is 1000 Hz. In addition to the sensor measurements, all relevant tamping parameters (Section 3.1) are also recorded at every tamping process. This allows a correct interpretation of the measurement data, which to a certain extent correlate with the applied machine settings (e.g., the applied squeezing pressure affects the measured squeezing force in the tamping tines).

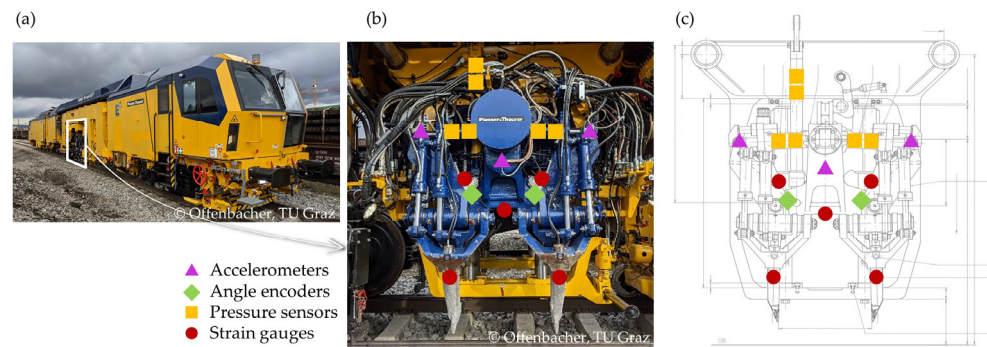


Figure 5. (a) Tamping machine Unimat 09-4x4/4S E³ and (b,c) measurement equipment installed on its four tamping unit segments.

The high quantity of measured parameters combined with the sample rate of 1000 Hz yields a large amount of raw data at every tamping process. Therefore, we calculated meaningful parameters from the raw measurements of each sensor for each relevant phase of the squeezing process (Section 3), i.e., ballast penetration and squeezing movement. These calculated parameters are a compressed expression of the raw measurements and reduce the data volume drastically, while significantly fostering statistical analyses.

Figure 6 displays examples of the tamping machine measurements. Plot (a) depicts the squeezing distance of one tamping arm during one squeezing movement. The plot includes raw measurements, low-pass filtered data, and the calculated parameters: the maximum squeezing distance and the x-coordinate of the centre of gravity of the area beneath the curve up to the tamping arms point of return. This parameter indicates the deceleration of the tamping arm during the squeezing movement. Plot (b) of Figure 6 depicts the squeezing force (normal force in one tamping tine) during a squeezing movement. Once again, the plot includes raw measurements, low-pass filtered data, and the derived parameters, which in this case are the average low-pass filtered squeezing force during the squeezing movement and the highest dynamic squeezing force.

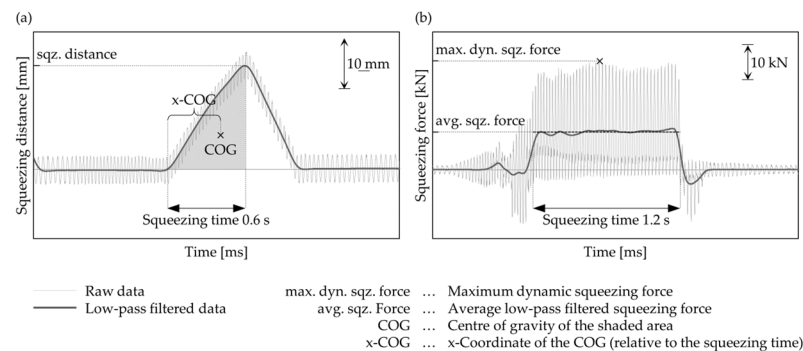


Figure 6. (a) Raw measurements and low-pass filtered data of the squeezing distance and (b) squeezing force and calculated parameters; the data originate from two different squeezing processes.

As all tamping unit segments, tamping arms, and tamping tines of the Unimat 09-4x4/4S E³ are equipped with sensors, every measurement parameter is recorded at multiple positions per sleeper. Consequently, all parameters calculated from the raw data (squeezing distance, centre of gravity of the squeezing distance, average low-pass filtered squeezing force, maximum dynamic squeezing force) are also available severalfold. These calculated values are averaged to one per tamping unit segment (left outside, left inside, right inside, right outside), yielding four values per measurement parameter, sleeper, and squeezing process phase.

In a next step, the calculated parameters are checked for outliers; these may either originate from measurement errors or from inconsistencies during the tamping process (e.g., if the tamping unit is not positioned perfectly central above the sleeper and a tamping

arm is consequently blocked by the sleeper). An algorithm developed for this purpose spans a moving window over three consecutive sleepers, thus covering twelve data points. If an individual data point of the middle sleeper (Sleeper 2 in Figure 7) deviates excessively from the median (the cut-off level is set at 0–2.5 times the median) of all twelve data points, it is removed. This procedure ensures that only values which approximately match their surrounding values are deemed reliable and used in further analyses. The arguably large, tolerated range of 0–2.5 times the median is necessary as even the averaged values may scatter considerably, depending on the local track condition.

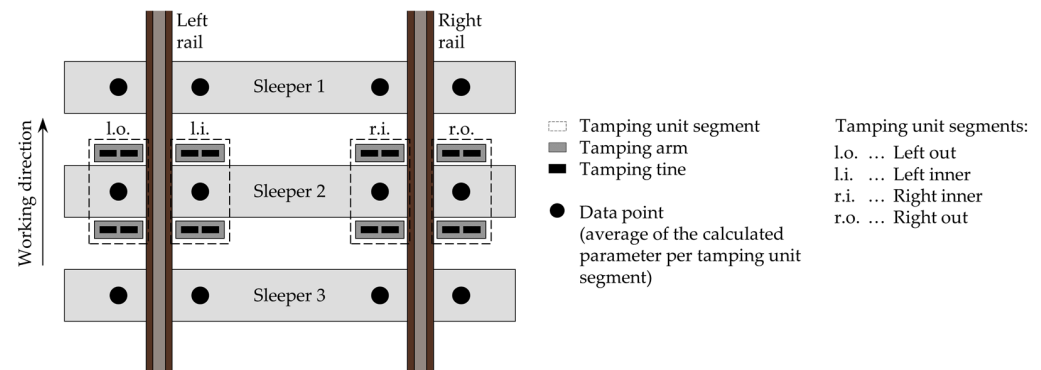


Figure 7. Illustration of the outlier detection algorithm.

4.2. Track Geometry Data Preparation

To analyse the track behaviour and assess the impact of a tamping operation, it is necessary to define which geometry parameter (Section 2) is analysed and which track quality index (Section 2.1) applied. Arguably the best suited and most frequently used track geometry parameter for this task is the longitudinal level D1 [22,25]. The wavelength range 3–25 m is particularly well suited as it is most affected by tamping [2]. The most commonly applied track quality index is the standard deviation (of the longitudinal level) [1,16,22]. Neuhold [9] analysed 20 years of track data of the Austrian railway network; this network represents the core of our investigations, too. In accordance with above mentioned researchers, Neuhold stated that the (modified) standard deviation [18,47] of the vertical track geometry, calculated with a moving window, is the best parameter to describe the track behaviour and the effect of tamping operations. Accordingly, the analyses of this study are also based on the standard deviation of the longitudinal level in the wavelength range D1 (3–25 m).

Since we aim to analyse the effect of tamping operations on the track behaviour as precisely as possible, the influence length of the standard deviation needs to be as short as possible. A graphical approach to determine a reasonable minimum influence length is presented in Figure 8. The plot depicts the two confining wave lengths of the D1 signal: (a) lower limit 3 m and (b) upper limit 25 m. Below, standard deviations of the respective signal calculated with different window lengths—100, 25, and 10 m—are plotted. Assuming that a track geometry signal with a constant amplitude represents a homogeneous track quality, the standard deviation should represent this through a near constant value. Accordingly, the graphs in Figure 8 indicate that the window for calculating the standard deviation should at least cover one wave length, which in case of the D1 signal equals 25 m. In case the window length of the standard deviation is shorter than the signal wave length, the standard deviation takes on low values where the signal features minima or maxima and high values at its inflection points. Consequently, we used a window length of 25 m to calculate the standard deviation of the longitudinal level D1.

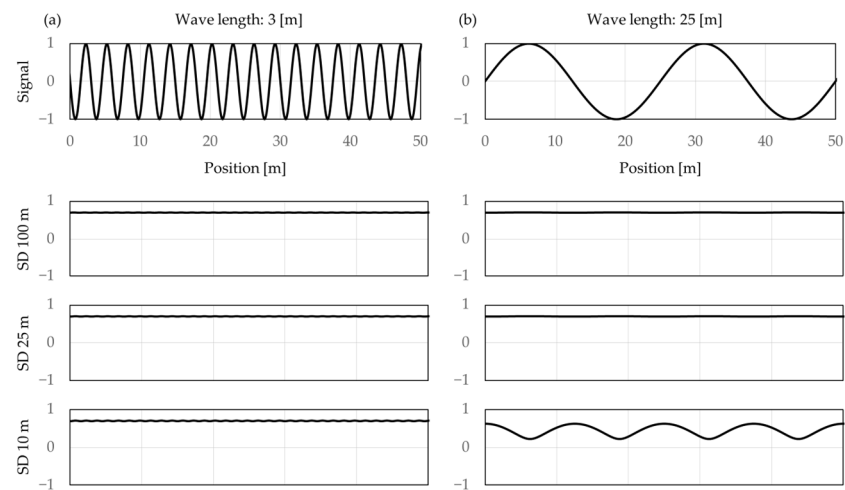


Figure 8. (a) Three metre sine wave and (b) 25 m sine wave and respective standard deviations with influence lengths of 100, 25, and 10 m.

Analysing time series of the standard deviation calculated with short windows requires accurately synchronised measurement signals. The signal positioning accuracy delivered by measuring vehicles, such as the EM250 used by OeBB, is generally sufficient for analyses of 200 or 100 m long track segments. In our case, however, a post processing method is necessary to improve signal synchronicity. For this purpose, a synchronisation method based on Fellingner’s CoMPAcT algorithm [48] is applied. The algorithm selects the most recent measurement signal, which is used as reference and fixed in its position, and shifts the next oldest signal until the Euclidian distance between both signals reaches a minimum. This process is repeated for all available measurement signals. According to Fellingner [48], the CoMPAcT algorithm delivers a synchronisation accuracy of one data break, which in case of the longitudinal level signal of the EM250 equals 0.25 m. An exemplary result of this synchronisation process is plotted in Figure 9.

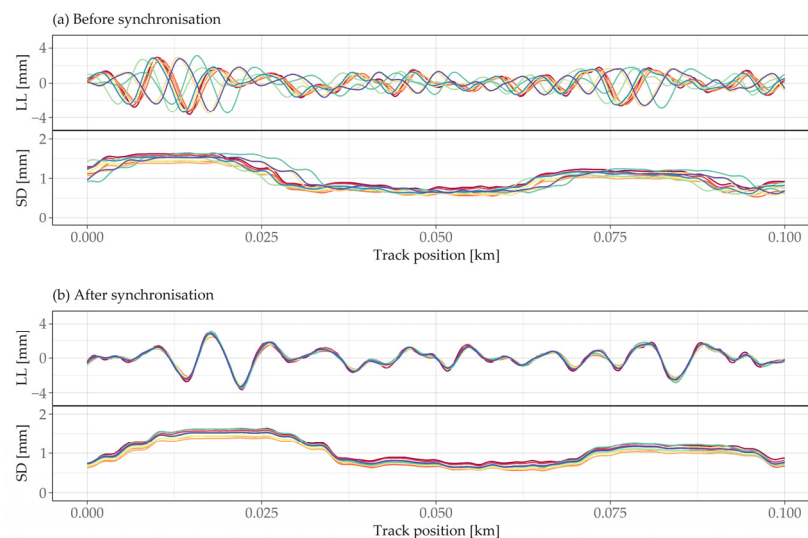


Figure 9. Longitudinal level (LL) D1 signals and standard deviations (SD) calculated with a moving window over 25 m; (a) before, (b) after the synchronisation process. Each colour represents an individual measurement run.

4.3. Linking Tamping Machine Measurements to Track Geometry Data

The tamping machine measurements are recorded at every sleeper, which are generally spaced at intervals of 0.6 m. These data points need to be allocated to the precise location

on the track, which is a precondition for reliable correlation analyses between tamping data and track behaviour. This mapping is achieved in a two-stage process: (i) First, the tamping data is merged with the tamping machine's internal measuring system for track geometry documentation ("DRP"; data recording processor). A DRP file includes the track position, the displacement of the track panel (lifting and shifting), and a control measurement of the established track geometry at a sampling rate of 0.5 m. The lift of the track panel is a parameter that is recorded by both the experimental measurement setup at the tamping unit and the DRP, hence, the lift can be used to synchronise these two data arrays. Due to the different sample rates of 0.6 m (tamping data) and 0.5 m (DRP) it is necessary to insert a common "virtual" sampling rate. This is achieved by adding virtual measurement points (e.g., every five centimetres) and linearly interpolating missing values between the original data points. Having established a common sampling rate, the lifting values of the tamping data file can be synchronised with the lifting values of the DRP file (Figure 10). Similar to Fellingner's synchronisation algorithm described above, one parameter is fixed and the other is shifting until the Euclidian distance between both curves reaches a minimum. As the DRP file includes the track position at every sampling point, the sleeper-specific tamping data are then also linked to the precise location on the track where the individual tamping processes were conducted.

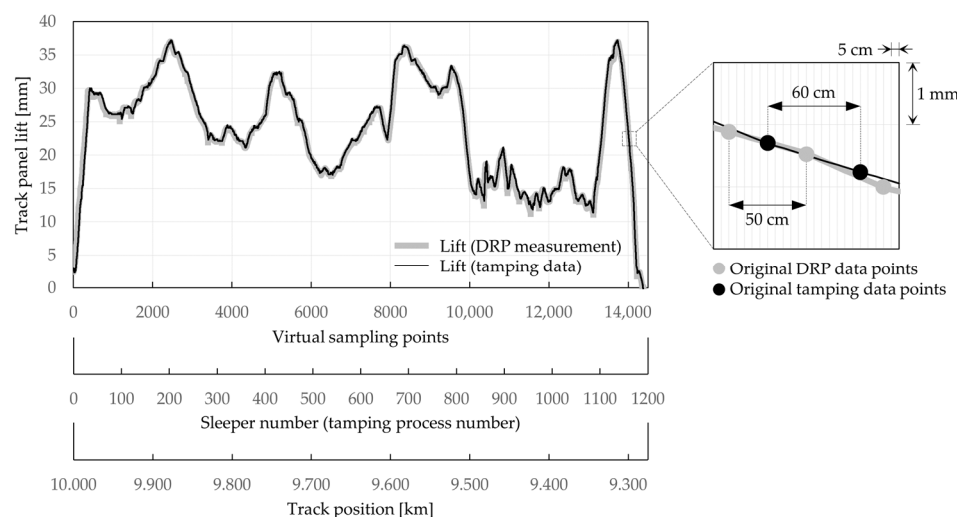


Figure 10. Merging process of sleeper-specific tamping data with the DRP control measurement.

(ii) In a second step, the combined data set (tamping data and DRP data) needs to be linked to the track geometry measurements of the infrastructure manager. This is achieved using the longitudinal level signals. The tamping machine measures the geometry of the corrected track with a steel cord and provides values every 0.5 m. In contrast, track recording vehicles rely on an inertial measuring unit (IMU) [48] providing measurement data every 0.25 m. Although the cord measurement is not identical to the IMU measurement, the longitudinal level signal of the DRP bears a close enough resemblance with the longitudinal level of the track recording vehicle to use it as a linking element between tamping machine data and track geometry data. The issue of non-matching sampling rates is again resolved by introducing virtual data points every 0.05 m and filling the created data gaps through linear interpolation. The track geometry data set—consisting of synchronised longitudinal level D1 signals and their respective standard deviations over 25 m—is filtered for the first track recording vehicle run after the tamping operation. The longitudinal level D1 signal of this measurement run matches the longitudinal level of the DRP's control measurement best. These two signals are combined using the track position information of the track recording vehicle and the position of the tamping machine (Figure 11a). Then, the DRP signal (together with all other parameters of the DRP file) is shifted until the sum of the Euclidian distances to the longitudinal level of the track

recording vehicle reaches a minimum (Figure 11b). Consequently, all DRP parameters recorded during tamping are accurately joined with the track geometry data set. The synchronisation logic is based on the CoMPAcT algorithm [48]; in this application, the accuracy of one data break equals 0.5 m (sample rate of the DRP).

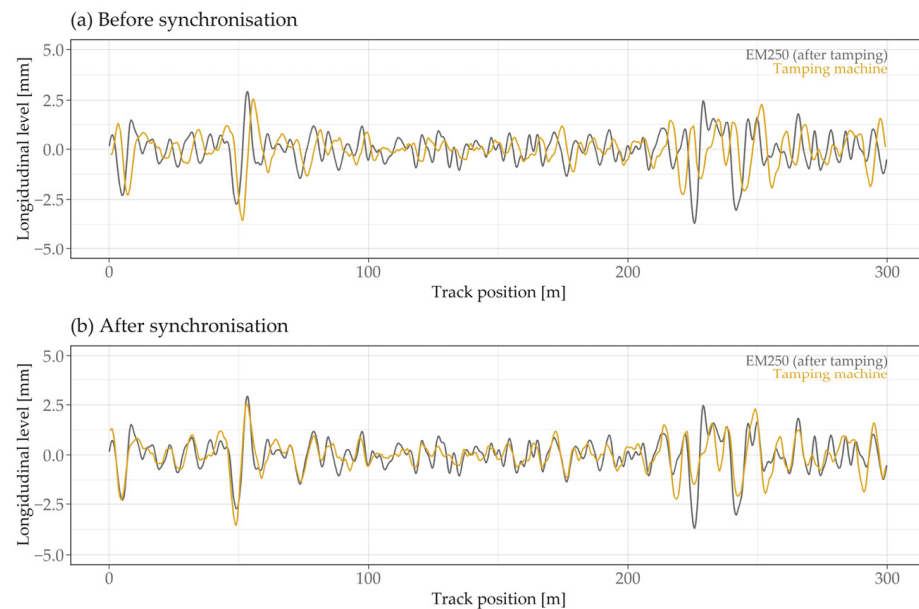


Figure 11. Merging tamping data and track geometry data by means of longitudinal level measurements; (a) before, (b) after the synchronisation process.

5. Conclusions and Outlook

This paper presents a methodology aimed at combining tamping machine data and track geometry data. The developed method provides the groundwork to correlate tamping process measurements and track behaviour for the first time. The result of the data preparation, data synchronisation, and data merging process described in Section 4 is a comprehensive data base which contains all required information for our intended investigations. It is planned to convert selected tamping machine measurement parameters—dynamic forces in the tamping tines, squeezing and compaction energy, squeezing movement (squeezing distance, centre of gravity of the squeezing distance)—into a “squeezing index”, which can be interpreted as a ballast compaction indicator.

The plausibility of the tamping process measurements can be illustrated by another application: Data recorded during the ballast penetration process (lowering movement of the tamping tines; Figure 4) by the same measurement setup (Figure 5) can be used to indicate the general condition of the bedding. For example, the maximum penetration force (vertical force in the tamping tines) extracted from the raw data shows a strong connection with the prevailing ballast condition (evaluated through extracted ballast samples and laboratory analyses; Figure 12). [49] This utilisation of the measurements demonstrates the suitability of the recorded data for our intended correlation analyses between squeezing index and track behaviour.

Besides the squeezing index, machine operator settings are also recorded, as this information will be used to cluster the tamping processes into groups of similar attributes which can be analysed collectively. If, for example, the number of squeezing movements per tamping process varies, the measurement values will become (partly) incomparable. Describing the track geometry via the standard deviation of the longitudinal level D1 with a window length of only 25 m enables the most accurate track behaviour analyses. We plan to investigate the effectiveness of the tamping operation on a relative basis, i.e., the track quality and track geometry deterioration rate after the tamping operation is set in relation to the quality and deterioration rate before tamping. Thus, a detailed clustering of track

parameters such as line speed, track load, curvature, and superstructure type can be omitted. This approach is valid for maintenance tamping, which constitutes the overwhelming majority of all tamping operations. Tamping during track reconstruction must be analysed separately, as all information on the track behaviour before reconstruction becomes invalid. The tamping machine providing the input data for this study (Unimat 09-4x4/4S E³) is regularly deployed for track maintenance, thus our data base is constantly expanded. While the machines' main area of operation is Austria, tamping works have also been conducted in Switzerland and Sweden; further foreign deployments are planned in the near future.

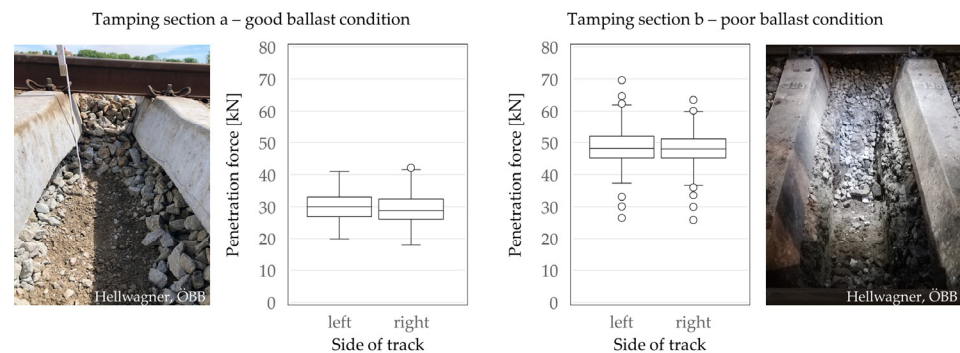


Figure 12. Application of the tamping machine measurements: Ballast condition assessment (penetration force per tamping tine; modified from [48]).

The presented methodology provides the foundation for in-depth analyses of the effect of individual tamping processes and the ballast condition on the quality and stability of the created track geometry. Our intended upcoming analyses based upon the established data set combine the advantages of highly specific and detailed measurements of the tamping process (over 200 measurement parameters; sample rate up to 1000 Hz) with a large-scale measurement campaign (the recording of the tamping data starts automatically at every tamping operation). Integrated evaluations of the quality and deterioration of an individual cross section with information on the latest tamping process and the indication for the ballast compaction at this location will significantly foster our understanding of the track behaviour. In future, this understanding can be converted into a better planning of tamping operations and higher automation level of the tamping process, where tamping parameters are automatically adapted to the prevailing boundary conditions. Consequently, a more accurate and more durable track geometry can be expected, leading to higher track availability and lower life cycle costs.

Author Contributions: Conceptualisation, S.O., C.K., M.L. and S.M.; methodology, S.O.; software, S.O.; validation, S.O. and C.K.; formal analysis, S.O.; investigation, S.O. and C.K.; resources, C.K., M.L. and S.M.; data curation, C.K.; writing—original draft preparation, S.O.; writing—review and editing, C.K., M.L. and S.M.; visualisation, S.O. and C.K.; supervision, S.M.; project administration, M.L.; funding acquisition, M.L. and S.M. All authors have read and agreed to the published version of the manuscript.

Funding: Open Access Funding by Graz University of Technology.

Institutional Review Board Statement: Not applicable.

Informed Consent Statement: Not applicable.

Data Availability Statement: Not applicable.

Acknowledgments: The authors would like to thank Plasser & Theurer, Austrian Federal Railways, and Swiss Federal Railways for the technical and financial support which they provided during this project.

Conflicts of Interest: The authors declare no conflict of interest.

References

1. Forschungs- und Versuchsamt des Internationalen Eisenbahnwesens (ORE). *Frage D 161.1: Dynamische Auswirkungen auf Das Gleis Infolge 22,5 t Radsatzlast—Bericht Nr. 4: Dynamische Auswirkungen der Anhebung der Radsatzlast von 20 auf 22,5 t und der geschätzte Anstieg der Oberbauerhaltungskosten*; Forschungs- und Versuchsamt des Internationalen Eisenbahnwesens (ORE): Utrecht, The Netherlands, 1987.
2. Forschungs- und Versuchsamt des Internationalen Eisenbahnwesens (ORE). *Frage D 161: Dynamische Erscheinungen der Wechselwirkung Fahrzeug/Gleis, aus der Sicht der Gleisunterhaltung—Bericht Nr. 3: Schlussbericht, Schlussfolgerungen und Empfehlungen*; Forschungs- und Versuchsamt des Internationalen Eisenbahnwesens (ORE): Utrecht, The Netherlands, 1988.
3. Caetano, L.F.; Teixeira, P.F. Optimisation model to schedule railway track renewal operations: A life-cycle cost approach. *Struct. Infrastruct. Eng.* **2014**, *11*, 1524–1536. [[CrossRef](#)]
4. Przybylowicz, M.; Sysyn, M.; Kovalchuk, V.; Nabochenko, O.; Parneta, B. Experimental and Theoretical Evaluation of Side Tamping Method for Ballasted Railway Track Maintenance. *Transp. Probl.* **2020**, *15*, 93–106. [[CrossRef](#)]
5. Neuhold, J.; Landgraf, M.; Marschnig, S.; Veit, P. Measurement Data-Driven Life-Cycle Management of Railway Track. *Transp. Res. Rec. J. Transp. Res. Board* **2020**, *2674*, 685–696. [[CrossRef](#)]
6. Vale, C.; Ribeiro, I.M.; Calçada, R. Integer programming to optimize tamping in railway tracks as preventive maintenance. *J. Transp. Eng.* **2012**, *138*, 123–131. [[CrossRef](#)]
7. Caetano, F.; Teixeira, P.F. Predictive maintenance model for ballast tamping. *J. Transp. Eng.* **2016**, *142*, 04016006. [[CrossRef](#)]
8. Bakhtiary, A.; Zakeri, J.A.; Mohammadzadeh, S. An opportunistic preventive maintenance policy for tamping scheduling of railway tracks. *Int. J. Rail Transp.* **2020**, *9*, 1–22. [[CrossRef](#)]
9. Neuhold, J. *Tamping within Sustainable Track Asset Management*; Verlag der Technischen Universität Graz: Graz, Austria, 2020.
10. Martey, E.N.; Attoh-Okine, N. Modeling tamping recovery of track geometry using the copula-based approach. *Proc. Inst. Mech. Eng. Part F J. Rail Rapid Transit* **2018**, *232*, 2079–2096. [[CrossRef](#)]
11. Audley, M.; Andrews, J.D. The effects of tamping on railway track geometry degradation. *Proc. Inst. Mech. Eng. Part F: J. Rail Rapid Transit* **2013**, *227*, 376–391. [[CrossRef](#)]
12. *EN 13848-1; Railway Applications—Track—Track Geometry Quality—Part 1: Characterization of Track Geometry*. Austrian Standards Institute: Vienna, Austria, 2019.
13. *EN 13848-5; Railway Applications—Track—Track Geometry Quality—Part 5: Geometrical Quality Levels—Plain Line, Switches and Crossings*. Austrian Standards Institute: Vienna, Austria, 2017.
14. Sadeghi, J. Development of Railway Track Geometry Indexes Based on Statistical Distribution of Geometry Data. *J. Transp. Eng.* **2010**, *136*, 693–700. [[CrossRef](#)]
15. Liu, R.-K.; Xu, P.; Sun, Z.-Z.; Zou, C.; Sun, Q.-X. Establishment of Track Quality Index Standard Recommendations for Beijing Metro. *Discret. Dyn. Nat. Soc.* **2015**, *2015*, 473830. [[CrossRef](#)]
16. Offenbacher, S.; Neuhold, J.; Veit, P.; Landgraf, M. Analyzing Major Track Quality Indices and Introducing a Universally Applicable TQI. *Appl. Sci.* **2020**, *10*, 8490. [[CrossRef](#)]
17. *EN 13848-6; Railway Applications—Track—Track Geometry Quality—Part 6: Characterisation of Track Geometry Quality*. Austrian Standards Institute: Vienna, Austria, 2014.
18. Neuhold, J.; Vidovic, I.; Marschnig, S. Preparing Track Geometry Data for Automated Maintenance Planning. *J. Transp. Eng. Part A: Syst.* **2020**, *146*, 04020032. [[CrossRef](#)]
19. BB-Infrastruktur AG. *Instandhaltungsplan Oberbauanlagen*; BB-Infrastruktur AG: Vienna, Austria, 2017; pp. 1–57.
20. SBB. *Einbau, Kontrollen und Unterhalt von Gleisen*, no. 4161906; SBB: Bern, Switzerland, 2020; pp. 1–23.
21. Hansmann, F.; Nemetz, W.; Spoors, R. *Keeping Track of Track Geometry*, 1st ed.; PMC Media House GmbH: Leverkusen, Germany, 2021.
22. Sauni, M.; Luomala, H.; Kolisoja, P.; Nummi, T. Advancing Railway Asset Management Using Track Geometry Deterioration Modeling Visualization. *J. Transp. Eng. Part A Syst.* **2022**, *148*, 1–12. [[CrossRef](#)]
23. Marschnig, S.; Fellinger, M.; Kumar, N.; Six, K. Zum Verhalten von Einzelfehlern der Gleislage. *ZE Vrail* **2022**, *146*, 91–97.
24. ElKhoury, N.; Hithamillage, L.; Moridpour, S.; Robert, D. Degradation Prediction of Rail Tracks: A Review of the Existing Literature. *Open Transp. J.* **2018**, *12*, 88–104. [[CrossRef](#)]
25. Soleimanmeigouni, I.; Ahmadi, A.; Kumar, U. Track geometry degradation and maintenance modelling: A review. *Proc. Inst. Mech. Eng. Part F: J. Rail Rapid Transit* **2016**, *232*, 73–102. [[CrossRef](#)]
26. Soleimanmeigouni, I.; Ahmadi, A.; Nissen, A.; Xiao, X. Prediction of railway track geometry defects: A case study. *Struct. Infrastruct. Eng.* **2019**, *16*, 987–1001. [[CrossRef](#)]
27. Offenbacher, S.; Antony, B.; Barbir, O.; Auer, F.; Landgraf, M. Evaluating the applicability of multi-sensor equipped tamping machines for ballast condition monitoring. *Measurement* **2020**, *172*, 108881. [[CrossRef](#)]
28. Barbir. *Development of Condition-Based Tamping Process in Railway Engineering—Operating Phases and Motion Behavior, Ballast Condition Determination, Ballast fluidization*; TU Wien: Vienna, Austria, 2022.
29. Zaayman, L. Chapter 6—Track Lifting, Levelling, Aligning and Tamping. In *Mechanisation of Track Work in Developing Countries*, 1st ed.; De Rooi Publications: Utrecht, The Netherlands, 2003; pp. 136–165.
30. *EN 13231-1; Railway Applications—Infrastructure—Acceptance of Works—Part 1: Works on Ballasted Track—Plain Line, Switches and Crossings*. Austrian Standards Institute: Vienna, Austria, 2022.
31. Lichtberger, B. *Track Compendium*, 2nd ed.; DVV Media Group GmbH I Eurailpress: Hamburg, Germany, 2011.

32. Zaayman, L. *The Basic Principles of Mechanised Track Maintenance*, 3rd ed.; PMC Media House GmbH: Bingen am Rhein, Germany, 2017.
33. Fischer, J. *Einfluss von Frequenz und Amplitude auf die Stabilisierung von Oberbauschotter*; Graz University of Technology: Graz, Austria, 1983.
34. Zhou, T.; Hu, B.; Sun, J.; Liu, Z. Discrete Element Method Simulation of Railway Ballast Compactness During Tamping Process. *Open Electr. Electron. Eng. J.* **2013**, *7*, 103–109. [[CrossRef](#)]
35. Omerović, S.; Daxberger, H.; Koczwar, C.; Antony, B.; Auer, F. *Anwendung der Diskrete-Elemente-Methode im Eisenbahnbau*; Ei—Der Eisenbahningenieur: Hamburg, Germany, 2021; pp. 39–41.
36. Saussine, G.; Azéma, E.; Perales, R.; Radjai, F. Compaction of Railway Ballast During Tamping Process: A Parametric Study. *AIP Conf. Proc.* **2009**, *1145*, 469–472. [[CrossRef](#)]
37. Sysyn, M.; Kovalchuk, V.; Gerber, U.; Nabochenko, O.; Pentsak, A. Experimental study of railway ballast consolidation inhomogeneity under vibration loading. *Pollack Period.* **2020**, *15*, 27–36. [[CrossRef](#)]
38. Barbir, O.; Antony, B.; Kopf, F.; Pistor, J.P.; Adam, D.; Auer, F. Compaction energy as an indicator for ballast quality. In Proceedings of the 12th World Congress on Railway Research, Tokyo, Japan, 28 October–1 November 2019; pp. 1–6.
39. Sysyn, M.; Nabochenko, O.; Kovalchuk, V.; Gerber, U. Evaluation of Railway Ballast Layer Consolidation after Maintenance Works. *Acta Polytech.* **2019**, *59*, 77–87. [[CrossRef](#)]
40. Liu, J.; Wang, P.; Liu, G.; Xiao, J.; Liu, H.; Gao, T. Influence of a tamping operation on the vibrational characteristics and resistance-evolution law of a ballast bed. *Constr. Build. Mater.* **2019**, *239*, 117879. [[CrossRef](#)]
41. Przybyłowicz, M.; Sysyn, M.; Gerber, U.; Kovalchuk, V.; Fischer, S. Comparison of the effects and efficiency of vertical and side tamping methods for ballasted railway tracks. *Constr. Build. Mater.* **2021**, *314*, 125708. [[CrossRef](#)]
42. Ilinykh, A.; Manakov, A.; Abramov, A.; Kolarzh, S. Quality assurance and control system for railway track tamping. *MATEC Web Conf.* **2018**, *216*, 03004. [[CrossRef](#)]
43. Zhou, T.; Hu, B.; Sun, J. Study of Railway Ballast Compactness under Tamping Operation. *J. Appl. Sci.* **2013**, *13*, 2072–2076. [[CrossRef](#)]
44. Barbir, O.; Adam, D.; Kopf, F.; Pistor, J.; Auer, F.; Antony, B. Development of condition-based tamping process in railway engineering. *ce/papers* **2018**, *2*, 969–974. [[CrossRef](#)]
45. Shi, S.; Gao, L.; Cai, X.; Yin, H.; Wang, X. Effect of tamping operation on mechanical qualities of ballast bed based on DEM-MBD coupling method. *Comput. Geotech.* **2020**, *124*, 103574. [[CrossRef](#)]
46. Hummitzsch, R. *Zur Prognostizierbarkeit des Qualitätsverhaltens von Gleisen: Statistische Analyse des Gleisverhaltens zur Erstellung eines Prognosemodells*; TU Graz: Graz, Austria, 2009.
47. Auer, F. *Gleislagequalitätsanalyse zur Instandhaltungsoptimierung*; ETR—Eisenbahntechnische Rundschau: Berlin, Germany, 2004; Volume 1, pp. 838–844.
48. Fellinger, M. *Sustainable Asset Management for Turnouts—From Measurement Data Analysis to Behaviour and Maintenance Prediction*; Graz University of Technology: Graz, Austria, 2020.
49. Offenbacher, S.; Landgraf, M.; Marschnig, S.; Antony, B.; Koczwar, C. Ballast condition monitoring with tamping machines. In Proceedings of the World Congress on Railway Research, Birmingham, UK, 6–10 June 2022; pp. 1–6.

Disclaimer/Publisher’s Note: The statements, opinions and data contained in all publications are solely those of the individual author(s) and contributor(s) and not of MDPI and/or the editor(s). MDPI and/or the editor(s) disclaim responsibility for any injury to people or property resulting from any ideas, methods, instructions or products referred to in the content.